Inorganic Chemistry

Article

pubs.acs.org/IC

Weak Ferromagnetic Transition with a Dielectric Anomaly in Hexagonal $Lu_{0.5}Sc_{0.5}FeO_3$

Atsunobu Masuno,*[,†] Atsushi Ishimoto,[†] Chikako Moriyoshi,[‡] Naoaki Hayashi,[§] Hitoshi Kawaji,[∥] Yoshihiro Kuroiwa,[‡] and Hiroyuki Inoue[†]

[†]Institute of Industrial Science, The University of Tokyo, Meguro-ku, Tokyo 153-8505, Japan

[‡]Department of Physical Science, Hiroshima University, Higashi-Hiroshima, Hiroshima 739-8526, Japan

[§]Institute for Integrated Cell-Material Sciences, Kyoto University, Sakyo-ku, Kyoto 606-8501, Japan

[∥]Materials & Structures Laboratory, Tokyo Institute of Technology, Midori-ku, Yokohama 226-8503, Japan

ABSTRACT: $Lu_{1-x}Sc_xFeO_3$ ($0 \le x \le 1$) was synthesized by a conventional solid-state reaction. The hexagonal phase appeared at $0.4 \le x \le 0.6$, between the perovskite phase ($0 \le x \le 0.3$) and the bixbyite phase ($0.7 \le x \le 1$). Structural, magnetic, and dielectric properties of hexagonal $Lu_{0.5}Sc_{0.5}FeO_3$ were investigated. Synchrotron X-ray diffraction measurements revealed that the crystal structure of $Lu_{0.5}Sc_{0.5}FeO_3$ is isomorphic to hexagonal ferroelectrics $RMnO_3$ (R = rare earth ion) with a polar space group of $P6_3cm$. A weak ferromagnetic transition with a dielectric anomaly occurred at a much higher temperature (162 K) than those in hexagonal $RMnO_3$. Although remanent magnetization was observed below the transition temperature, it decreased to almost zero at 10 K. These results indicate a strong antiferromagnetic interaction between ground-state Fe^{3+} ions on the triangular lattice.

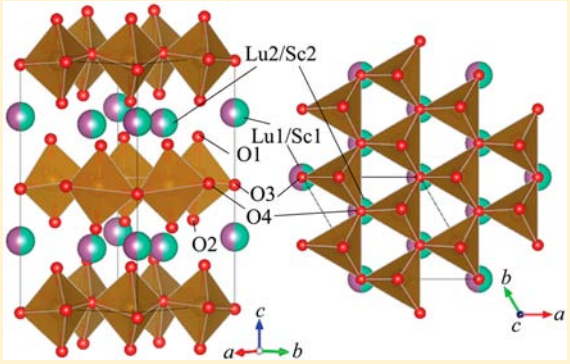

INTRODUCTION

Among the numerous oxides of chemical composition RMO_3 (R is a rare earth ion, M is a transition metal), hexagonal manganese oxides, $RMnO_3$, have attracted much attention owing to their fascinating properties of high-temperature ferroelectricity[1−5] and a magnetically frustrated structure.[6,7] The hexagonal structure consists of close-packed layers of trigonal MnO_5 bipyramids, where each Mn^{3+} ion is surrounded by three in-plane and two apical O^{2-} ions. The MnO_5 bipyramids share the in-plane oxygen ions to form a triangular lattice in the *ab* plane and are separated along the *c* axis by R layers. Ferroelectricity is geometric in origin, arising from the cooperative tilting of MnO_5 bipyramids and the buckling of R layers.[1] Recent studies have suggested that $RMnO_3$ ferroelectricity is driven by orbital hybridization between the R^{3+} and in-plane O^{2-} ions along the *c* axis.[3−5] The magnetic property is dominated by the antiferromagnetic interaction between the spins of the Mn^{3+} ions on the triangular lattice in the *ab* plane, which aligns the Mn moment into a 120° structure in the plane. The stacking of the triangular lattice planes renders the magnetic structure in hexagonal $RMnO_3$ a frustrated system.[6,7]

As is well known, the hexagonal phase of $RMnO_3$ appears when R is small (Ho−Lu, Y, or Sc), and the perovskite phase emerges at large R (La−Dy), indicating that the crystal structure stability strongly depends on the ionic radii of R. However, $RFeO_3$ prepared by conventional solid-state synthesis has a perovskite structure for R = rare earth regardless of the size of R. Hexagonal $RFeO_3$ has been prepared when R is small, and some material processes for metastable phase formation are used: nanoparticles (R = Eu, Yb) by the spray-ICP technique[8] and solution-based precursor methods,[9−14] thin films by low-pressure metal−organic chemical vapor deposition,[15] and pulsed laser deposition,[16−22] and bulk ceramics by containerless processing.[23,24] In hexagonal $RFeO_3$ thin films (R = Y, Yb, and Lu), room-temperature ferroelectricity has been confirmed in the presence of a polarization-field (PE) hysteresis loop, and an antiferromagnetic transition has been observed at approximately 120 K. These results demonstrate not only the rich functionality of hexagonal $RFeO_3$ as well as hexagonal $RMnO_3$ but also the comparable crystal structure stabilities of the hexagonal and perovskite phases as also observed in $RMnO_3$ when the size of R is small.[25,26]

Considering that the metastable phases of $RFeO_3$ (R is a small rare earth ion) are hexagonal, the hexagonal phase may appear even as a stable phase by decreasing the size of R. When R is Sc, whose size is smaller than that of Lu, the stable phase is not hexagonal but bixbyite.[27] However, the crystal phases of chemical compositions between $LuFeO_3$ and $ScFeO_3$, where the averaged R size is decreased by the substitution of Sc for Lu, are yet to be investigated. Thus, in this study, $Lu_{1-x}Sc_xFeO_3$ ($0 \le x \le 1$) was prepared by a conventional solid-state reaction,

Received: June 11, 2013
Published: September 30, 2013

   dx.doi.org/10.1021/ic401482h | *Inorg. Chem.* 2013, 52, 11889−11894

and the crystal structures were determined. It was found that the hexagonal phase appeared in the region of mid-x, between the perovskite and bixbyite phases. The crystal structure parameters of hexagonal $Lu_{0.5}Sc_{0.5}FeO_3$ were obtained from synchrotron X-ray diffraction data. The local structure and the chemical state of Fe in hexagonal $Lu_{0.5}Sc_{0.5}FeO_3$ were investigated by Mössbauer spectroscopy. The magnetic and dielectric properties of hexagonal $Lu_{0.5}Sc_{0.5}FeO_3$ were measured and compared to those of hexagonal $RMnO_3$.

EXPERIMENTAL PROCEDURES

High-purity Lu_2O_3, Sc_2O_3, and Fe_2O_3 powders were stoichiometrically mixed to yield $Lu_{1-x}Sc_xFeO_3$ ($0 \le x \le 1$). The mixed powders were pelletized and sintered at 1000 °C for 12 h and then at 1200 °C for 24 h in air with intermediate grindings.

High-energy synchrotron-radiation (SR) X-ray powder diffraction measurements of $Lu_{1-x}Sc_xFeO_3$ ($0 \le x \le 1$) were performed at room temperature using a large Debye−Scherrer camera installed at BL02B2 in SPring-8.[28] The sample was ground in an agate mortar and sealed in a glass capillary of internal diameter 0.1 mm. The SR wavelength was λ = 0.49608(7) Å. The crystal structures were analyzed by the Rietveld method using diffraction intensity data up to 45° in 2θ (d > 0.65 Å).

The physical properties of the x = 0.5 compound with hexagonal structure were investigated. Mössbauer spectroscopy was performed at room temperature in transmission geometry using a ^{57}Co/Rh source. Powder samples were pressed onto an aluminum foil. The velocity scale and the isomer shift were calibrated using α-Fe. The resulting spectra were least-squares fitted using the Lorentzian function. Magnetization measurements were carried out using a superconducting quantum interference device (SQUID, MPMS, Quantum Design) magnetometer. The magnetic susceptibility was measured over the temperature range of 5−300 K in a magnetic field of 1000 Oe, and the magnetic moments were measured under fields ranging from −50 000 to 50 000 Oe at 10, 105, and 300 K. The heat capacity measurements were performed using a physical property measurement system (PPMS, Quantum Design) under zero magnetic field. The temperature dependence of the dielectric properties was measured with an impedance analyzer (HP4194A, Hewlett-Packard) at an ac amplitude perturbation voltage of 100 mV in the frequency range of 1 kHz−1 MHz, where the sample was pelletized to a diameter of 5 mm and a thickness of 500 μm, and Au electrodes were sputtered on both sides of the pellet.

RESULTS AND DISCUSSION

Figure 1 shows the synchrotron X-ray diffraction (XRD) profiles of $Lu_{1-x}Sc_xFeO_3$. Single phases of perovskite $LuFeO_3$ and bixbyite $ScFeO_3$ were obtained at x = 0 and 1, respectively. As x increased from 0 to 0.5, the peak intensity originating from the perovskite phase decreased, whereas that from an unknown phase increased. With further increases in x from 0.5 to 1, the peak of the unknown phase decreased and those of the bixbyite phase emerged. The profile of the unknown phase at x = 0.5 was similar to that of metastable hexagonal $LuFeO_3$ prepared by containerless processing.[23,24]

Figure 2 shows the Rietveld profile fitting results of $LuFeO_3$, $Lu_{0.5}Sc_{0.5}FeO_3$, and $ScFeO_3$. The initial atomic coordinations of $LuFeO_3$ used are the reported structure parameters of the perovskite phase. The refined structural parameters are listed in Table 1. A crystal structure with noncentrosymmetric space group $P6_3cm$ (that of metastable $LuFeO_3$) was assumed for $Lu_{0.5}Sc_{0.5}FeO_3$.[23,24] There are weak peaks derived from minor phases whose amount is approximately 3%. The refined structure of $Lu_{0.5}Sc_{0.5}FeO_3$ is hexagonal with unit cell parameters a = 5.86024(6) Å, c = 11.7105(2) Å, and Z = 6. In the analysis, the thermal parameters of the O atoms are assumed to be identical. The obtained reliable factors (R factors) were small: R_{wp} = 4.90%, R_I = 2.58%, and R_F = 2.37%. Lattice parameter a of $Lu_{0.5}Sc_{0.5}FeO_3$ is significantly smaller than that of metastable $LuFeO_3$ (a = 5.96522(5) Å), and lattice parameter c of $Lu_{0.5}Sc_{0.5}FeO_3$ is slightly larger than that of metastable $LuFeO_3$ (c = 11.70219(2) Å).[23,24] The refined structural parameters with the z origin at the z coordinate of Fe are listed in Table 2. We have examined the possibility of a hexagonal structure with centrosymmetric space group $P6_3$/

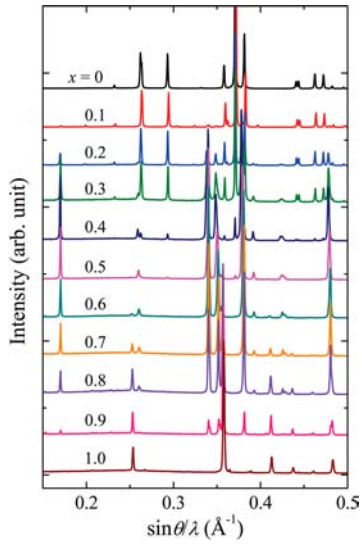

Figure 1. Synchrotron X-ray diffraction profiles of $Lu_{1-x}Sc_xFeO_3$. λ = 0.49608(7) Å.

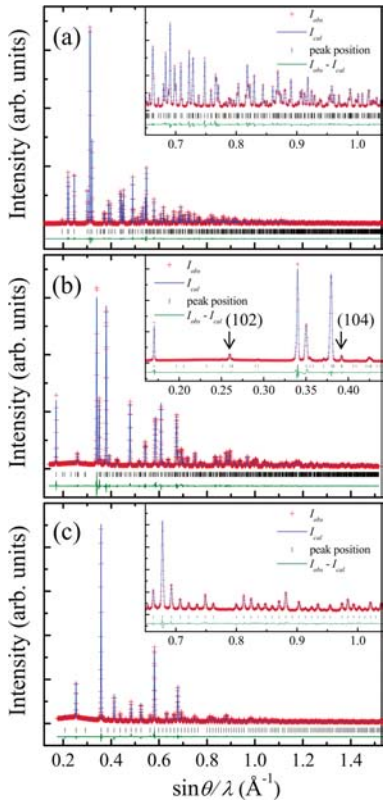

Figure 2. Rietveld profile fitting results for (a) $LuFeO_3$, (b) $Lu_{0.5}Sc_{0.5}FeO_3$, and (c) $ScFeO_3$. The deviation between the observed (+) and calculated (solid line) results is shown at the bottom of the graphs, with peak positions indicated. The insets show enlarged views.

dx.doi.org/10.1021/ic401482h | Inorg. Chem. 2013, 52, 11889−11894

Table 1. Refined Structural Parameters of Perovskite $LuFeO_3$ at 300 K[a]

atom	site	g	x	y	z	U (10^{-2} Å^2)
Lu	4c	1.0	0.07134(3)	0.25	0.97985(1)	0.44(3)
Fe	4b	1.0	0.5	0	0	0.46(2)
O1	4c	1.0	0.453(2)	0	0.120(5)	0.3(2)
O2	8d	1.0	0.308(3)	0.060(2)	0.689(2)	0.5(2)

[a]Space group *Pnma* (No. 62), $Z = 4$. Lattice parameters: $a = 5.5526$ Å, $b = 7.5601$ Å, and $c = 5.2115$ Å. $R_{wp} = 3.57\%$, $R_I = 1.98\%$, and $R_F = 2.06\%$.

Table 2. Refined Structural Parameters of Hexagonal $Lu_{0.5}Sc_{0.5}FeO_3$ at 300 K[a]

atom	site	g	x	y	z	U (10^{-2} Å^2)
Lu1/Sc1	2a	1.0	0	0	0.2698(1)	0.39(3)
Lu2/Sc2	4b	1.0	1/3	2/3	0.2342(4)	0.41(3)
Fe	6c	1.0	0.332(2)	0	0	0.29(2)
O1	6c	1.0	0.308(1)	0	0.1693(5)	0.7(2)
O2	6c	1.0	0.648(3)	0	0.334(2)	0.7(2)
O3	2a	1.0	0	0	0.4788(9)	0.7(2)
O4	4b	1.0	1/3	2/3	0.016(1)	0.7(2)

[a]Space group $P6_3cm$ (No. 185), $Z = 6$. Lattice parameters: $a = 5.86024(6)$ Å and $c = 11.7105(2)$ Å. $R_{wp} = 4.90\%$, $R_I = 2.58\%$, and $R_F = 2.37\%$.

mmc for $Lu_{0.5}Sc_{0.5}FeO_3$. In this space group, indices of type $(3n + 102m)$ are prohibited but are allowed in $P6_3cm$. As indicated by the arrows in Figure 2b, the possibility of $P6_3/mmc$ is precluded by the appearance of the weak (102) and (104) reflections. To date, metastable hexagonal $RFeO_3$ has been obtained in various forms, such as nanoparticles, thin films, and bulk ceramics. However, metastability may limit the applicability of a material. On the contrary, hexagonal $Lu_{0.5}Sc_{0.5}FeO_3$ remained stable even during annealing at 1300 °C for 24 h, which indicates that the compound has been obtained as a stable phase. The refined structural parameters of $ScFeO_3$ with the bixbyite structure are listed in Table 3. The site occupancies of Sc and Fe atoms are set to 0.5 for 24d and 8b sites, respectively.

Figure 3a–c shows the composition dependence of the lattice parameters of $Lu_{1-x}Sc_xFeO_3$ ($0 \le x \le 1$). Three regions with different main phases emerge: perovskite ($0 \le x \le 0.3$), hexagonal ($0.4 \le x \le 0.6$), and bixbyite ($0.7 \le x \le 1.0$). The lattice constants change linearly with increasing x in all three regions as Lu^{3+} is gradually substituted with Sc^{3+}. The composition dependence of the molar volume is shown in Figure 3d. The molar volumes of hexagonal phases are larger than those of cubic and orthorhombic phases. With increasing Sc content, the molar volume decreases in the three regions. The effect of Sc substitution on the molar volume in the hexagonal phase is larger than those of the cubic phase and orthorhombic phase.

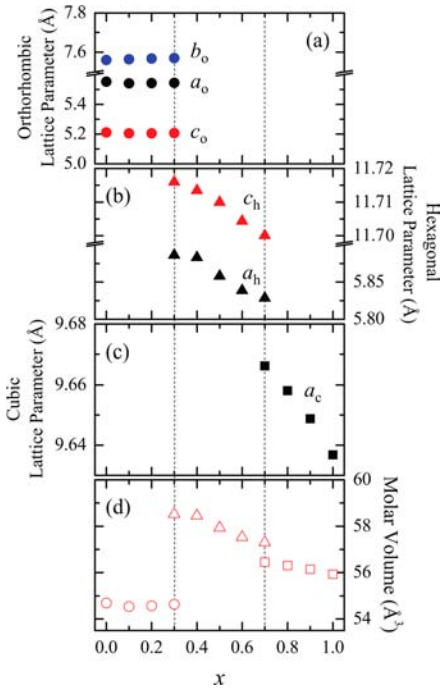

Figure 3. Composition dependence of lattice parameters of $Lu_{1-x}Sc_xFeO_3$ for (a) orthorhombic, (b) hexagonal, and (c) cubic structures. (d) Composition dependence of the molar volume.

Figure 4 shows the Mössbauer spectrum of $Lu_{0.5}Sc_{0.5}FeO_3$ at room temperature. The spectrum shows a single doublet although a weak sextet signal derived from minor phases was observed. The amount of the minor phases was estimated to be approximately 4% in atomic percentage of Fe, which corresponds to that estimated in the XRD profile. The single doublet is the evidence that there is one Fe site. This is

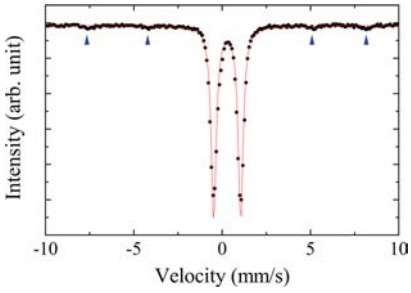

Figure 4. ^{57}Fe Mössbauer spectrum (solid circles) at room temperature and fitting results (lines) of hexagonal $Lu_{0.5}Sc_{0.5}FeO_3$. Signals from the minor phases are indicated by arrows.

Table 3. Refined Structural Parameters of Bixbyite $ScFeO_3$ at 300 K[a]

atom	site	g	x	y	z	U (10^{-2} Å^2)
Sc1	24d	0.5	0.96553(6)	0	0.25	0.110(4)
Fe1	24d	0.5	0.96553(6)	0	0.25	0.110(4)
Sc2	8b	0.5	0.25	0.25	0.25	0.85(2)
Fe2	8b	0.5	0.25	0.25	0.25	0.85(2)
O	48e	1.0	0.38627(7)	0.15706(9)	0.3801(1)	1.13(2)

[a]Space group *Ia*-3 (No. 206), $Z = 16$. Lattice parameter: $a = 9.6364(1)$ Å. $R_{wp} = 4.99\%$, $R_I = 4.40\%$, and $R_F = 3.38\%$.

dx.doi.org/10.1021/ic401482h | *Inorg. Chem.* 2013, 52, 11889–11894

consistent with the crystal structure determined by XRD analyses. The value of the isomer shift (IS = 0.28 mm/s) of the doublet corresponds to that of Fe^{3+} ($S = {}^5/_2$). However, two doublets with similar IS values were observed in the spectra of the hexagonal $RFeO_3$ synthesized by the solution method.[8,12,13] It was suggested that the two doublets might be caused by low crystallinity resulting from the synthesis process on the basis of the comparison with the spectrum of hexagonal $YIn_{0.7}Fe_{0.3}O_3$ prepared by high-temperature solid-state reactions.[12] This is supported by the results of hexagonal $Lu_{0.5}Sc_{0.5}FeO_3$. The relatively large quadrupole splitting (QS = 1.47 mm/s) may reflect the characteristic bipyramid oxygen coordination of Fe^{3+} of hexagonal $Lu_{0.5}Sc_{0.5}FeO_3$.

The temperature dependence of the molar magnetic susceptibility χ at 1000 Oe in the zero-field-cooled (ZFC) and field-cooled (FC) modes is shown in Figure 5a. In both

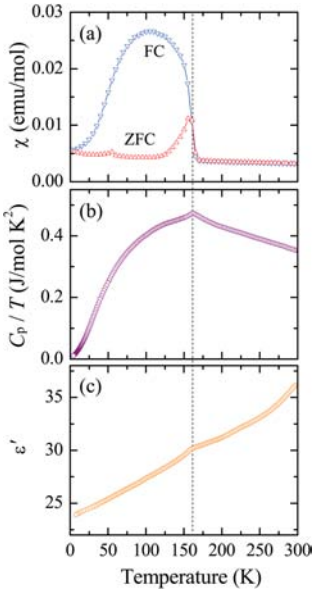

Figure 5. Temperature dependence of the (a) zero-field-cooled (ZFC) and field-cooled (FC) molar magnetic susceptibility χ at 1000 Oe, (b) the heat capacity divided by temperature, and (c) the dielectric constant ε' at 500 kHz for hexagonal $Lu_{0.5}Sc_{0.5}FeO_3$.

modes, magnetization increases rapidly at 165 K. The specific heat divided by temperature C_p/T exhibits an anomaly at 162 K as shown in Figure 5b, which is almost identical to the magnetic result. Therefore, the magnetic transition occurs at this temperature. The plot of C_p/T versus T^2 was fitted to the simple Debye model: $C_p = \gamma T + \beta T^3$ where γ and β are the coefficients of the electronic and lattice contributions to the specific heat, respectively. The values of γ and β are 6.7 mJ/mol K^2, and 0.24 mJ/mol K^4, respectively, and thus the Debye temperature Θ_D was estimated to be 343 K. The reported Debye temperatures are 350−420 K for heavy elements and 780−800 K for light elements, which were estimated on the basis of two Debye temperature models.[29]

It was found that the magnetic susceptibility obeys the Curie−Weiss law above the transition temperature from the reciprocal magnetic susceptibility as a function of temperature. Fitting the observed data to the Curie−Weiss formula, we determined Curie constant $\chi = C/(T - \Theta)$ and Weiss temperature Θ to be 2.93 emu/(mol K) and −614 K, respectively. The large negative Weiss temperature is characteristic of antiferromagnetic interactions. The ratio of Θ to the magnetic transition temperature, which is related to the degree of frustration, is estimated to be 3.7. The degree of frustration is smaller than that reported in hexagonal $RMnO_3$. The effective magnetic moment obtained from the Curie constant is 4.84μ_B/Fe, which is relatively smaller than 5.9μ_B, the value expected for a high-spin state of Fe^{3+} ($S = {}^5/_2$). The discrepancy between the experimental value and the theoretical value might be caused by the small quantity of impurities, or the temperature range for the fitting might be too low compared to the Weiss temperature.[29]

Note that the magnetic transition temperature of $Lu_{0.5}Sc_{0.5}FeO_3$ is the highest among hexagonal $RMnO_3$ and metastable hexagonal $RFeO_3$.[6,7] The critical factor affecting the magnetic transition temperature of hexagonal $RMnO_3$ has been previously elucidated. In a hexagonal lattice, as the lattice parameter a decreases, the value of the exchange integral J characterizing the superexchange interaction in the ab plane between Mn^{3+} ions increases. Indeed, in the $Lu_{1-x}Sc_xMnO_3$ solid-solution system, the magnetic transition temperature increases from 92 to 133 K as x increases.[30] Furthermore, substituting Mn^{3+} with Fe^{3+} increases the magnetic transition temperature of $LuMn_{1-x}Fe_xO_3$ (up to $x \leq 0.2$).[31] As the compound is increasingly doped with Fe^{3+}, the exchange interaction is strengthened because Fe^{3+} possesses one more unpaired electron than does Mn^{3+}. Accordingly, the high magnetic transition temperature is realized in hexagonal $Lu_{0.5}Sc_{0.5}FeO_3$ because lattice parameter a shrinks as Lu^{3+} is replaced by Sc^{3+}, and the exchange interaction is enhanced by Fe^{3+} rather than Mn^{3+}.

Below the magnetic transition temperature, the ZFC curve is low-valued and almost constant, with a peak at 155 K. The FC curve shows a maximum at 100 K before declining to the level of the ZFC curve at 10 K. Because neither Lu^{3+} nor Sc^{3+} possesses a magnetic moment, these results imply that at lower temperatures the antiferromagnetic interaction between Fe^{3+} ions is greatly enhanced.

Figure 5c shows the temperature dependence of the dielectric constant (ε') of hexagonal $Lu_{0.5}Sc_{0.5}FeO_3$ at 500 kHz. As the temperature decreases, the dielectric constant decreases and kinks around 160 K, which is almost identical to the magnetic transition temperature. A similar dielectric anomaly has been reported in single crystals of hexagonal $YMnO_3$ and $LuMnO_3$.[6,7] The anomaly was seen with the electric field along the ab plane but was absent along the c axis. This result was attributed to a spin-dependent charge-transfer gap between Mn 3d and in-plane oxygen 2p states undergoing strong p−d exchange interactions. From detailed neutron-scattering experiments on hexagonal $RMnO_3$, it was revealed that all structural parameters change at the magnetic transition temperature, implying strong spin−lattice coupling and consequent magnetoelectric coupling. Accordingly, hexagonal $Lu_{0.5}Sc_{0.5}FeO_3$ should exhibit similar strong spin−lattice coupling, which might cause the dielectric anomaly.

The magnetic field dependence of the magnetization of hexagonal $Lu_{0.5}Sc_{0.5}FeO_3$ is shown in Figure 6. Measurements were conducted at 10, 105, and 300 K. A linear change was seen at 10 K because of the antiferromagnetic interaction and at 300 K because the magnetic order disappeared. A hysteresis loop appearing at 105 K indicates the existence of a weak ferromagnetic property. The coercive field is 6000 Oe, and the remanent magnetic moment is 0.0043μ_B. The hysteresis loop at 105 K might arise from a Dzyaloshinskii−Moriya

dx.doi.org/10.1021/ic401482h | Inorg. Chem. 2013, 52, 11889−11894

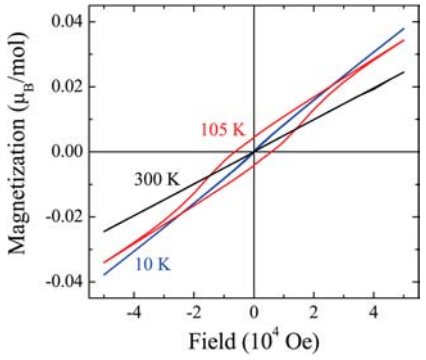

Figure 6. Magnetic field dependence of the magnetization of hexagonal $Lu_{0.5}Sc_{0.5}FeO_3$ at 10, 105, and 300 K.

interaction by the nonperfect triangular alignment of Fe^{3+} ions on the *ab* plane. Weak ferromagnetic behavior has also been reported in thin films of $YFeO_3$ and $LuFeO_3$.[18,22] In the case of the thin films, the ground-state Fe^{3+} spins were calculated to form a 120° triangular spin structure on the *ab* plane as well as on $YMnO_3$. In addition, they were found to be slightly canted with a magnetic moment of $0.0027\mu_B$ along the *c* direction. The weak ferromagnetic interaction increases with decreasing temperature in the thin films. Compared to the manganese thin films, the stronger antiferromagnetic interaction develops on the *ab* plane or along the *c* direction with decreasing temperature in hexagonal $Lu_{0.5}Sc_{0.5}FeO_3$.

SUMMARY

Hexagonal $Lu_{0.5}Sc_{0.5}FeO_3$ was prepared as a stable phase by a conventional solid-state reaction. Rietveld analysis demonstrated that the space group is $P6_3cm$ and the crystal structure is hexagonal with unit cell parameters a = 5.86024(6) Å, c = 11.7105(2) Å, and Z = 6. Mössbauer spectroscopy confirmed that there is one Fe site in the structure. A weak ferromagnetic transition occurred at 162 K, the highest reported transition temperature in a hexagonal $RMnO_3$ or $RFeO_3$ system. A dielectric constant anomaly was seen at the magnetic transition temperature, indicating that spin−lattice interactions occur at this temperature. Hexagonal $Lu_{0.5}Sc_{0.5}FeO_3$ therefore presents a promising magnetoelectric material with a magnetic transition temperature higher than that of the $RMnO_3$ system. Below the transition temperature, a hysteresis loop with a remanent magnetization of $0.0043\mu_B$ and a coercive field of 6000 Oe was observed. From the linear behavior of magnetization at 10 K, it was suggested that the strong antiferromagnetic interactions develop on the *ab* plane or along the *c* direction as the temperature decreases.

AUTHOR INFORMATION

Corresponding Author

*E-mail: masuno@iis.u-tokyo.ac.jp.

Notes

The authors declare no competing financial interest.

ACKNOWLEDGMENTS

The SR experiments were carried out with the approval of the Japan Synchrotron Radiation Research Institute (JASRI, proposal nos. 2008B1040 and 2010A1220). This research was partially granted by the Collaborative Research Project of the Materials and Structures Laboratory, Tokyo Institute of Technology. We thank Mr. Y. Okazaki for his experimental support at SPring-8.

REFERENCES

(1) Van Aken, B. B.; Palstra, T. T. M.; Filippetti, A.; Spaldin, N. A. *Nat. Mater.* **2004**, *3*, 164.
(2) Gibbs, A. S.; Knight, K. S.; Lightfoot, P. *Phys. Rev. B* **2011**, *83*, 094111.
(3) Cho, D.-Y.; Kim, J.-Y.; Park, B.-G.; Rho, K.-J.; Park, J.-H.; Noh, H.-J.; Kim, B. J.; Oh, S.-J.; Park, H.-M.; Ahn, J.-S.; Ishibashi, H.; Cheong, S.-W.; Lee, J. H.; Murugavel, P.; Noh, T. W.; Tanaka, A.; Jo, T. *Phys. Rev. Lett.* **2007**, *98*, 217601.
(4) Kim, J.; Sho, K. C.; Koo, Y. M.; Hong, K. P.; Shin, N. *Appl. Phys. Lett.* **2009**, *95*, 132901.
(5) Ahn, S.-J.; Kim, J.; Shin, N.; Koo, Y.-M. *J. Appl. Phys.* **2011**, *110*, 084112.
(6) Katsufuji, T.; Mori, S.; Masaki, M.; Moritomo, Y.; Yamamoto, N.; Takagi, H. *Phys. Rev. B* **2001**, *64*, 104419.
(7) Katsufuji, T.; Masaki, M.; Machida, A.; Moritomo, M.; Kato, K.; Nishibori, E.; Takata, M.; Sakata, M.; Ohoyama, K.; Kitazawa, K.; Takagi, H. *Phys. Rev. B* **2002**, *66*, 134434.
(8) Mizoguchi, Y.; Onodera, H.; Yamauchi, H.; Kagawa, M.; Syono, Y.; Hirai, T. *Mater. Sci. Eng.* **1996**, *A217/218*, 164.
(9) Yamaguchi, O.; Takemura, H.; Yamashita, M.; Hayashida, A. *J. Electrochem. Soc.* **1991**, *138*, 1492.
(10) Wu, L.; Yu, J. C.; Zhang, L.; Wang, X.; Li, S. *J. Solid State Chem.* **2004**, *177*, 3666.
(11) Liu, J.; Singh, U. G.; Schladt, T. D.; Stalick, J. K.; Scott, S. L.; Seshadri, R. *Chem. Mater.* **2008**, *20*, 6567.
(12) Jiang, P.; Li, J.; Sleight, A. W.; Subramanian, M. A. *Inorg. Chem.* **2011**, *50*, 5858.
(13) Downie, L. J.; Goff, R. J.; Kockelmann, W.; Forder, S. D.; Parker, J. E.; Morrison, F. D.; Lightfoot, P. *J. Solid State Chem.* **2012**, *190*, 52.
(14) Nishimura, T.; Hosokawa, S.; Masuda, Y.; Wada, K.; Inoue, M. *J. Solid State Chem.* **2013**, *197*, 402.
(15) Bossak, A. A.; Graboy, I. E.; Gorbenko, O. Y.; Kaul, A. R.; Kartavtseva, M. S.; Svetchnikov, V. L.; Zandbergen, H. W. *Chem. Mater.* **2004**, *16*, 1751.
(16) Akbashev, A. R.; Semisalova, A. S.; Perov, N. S.; Kaul, A. R. *Appl. Phys. Lett.* **2011**, *99*, 122502.
(17) Iida, H.; Koizumi, T.; Uesu, Y.; Kohn, K.; Ikeda, N.; Mori, S.; Haumont, R.; Janolin, P.-E.; Kiat, J.-M.; Fukunaga, M.; Noda, Y. *J. Phys. Soc. Jpn.* **2012**, *81*, 024719.
(18) Jeong, Y. K.; Lee, J.-H.; Ahn, S.-J.; Song, S.-W.; Jang, H. M.; Choi, H.; Scott, J. F. *J. Am. Chem. Soc.* **2012**, *134*, 1450.
(19) Jeong, Y. K.; Lee, J.-H.; Ahn, S.-J.; Jang, H. M. *Chem. Mater.* **2012**, *24*, 2426.
(20) Pavlov, V. V.; Akbashev, A. R.; Kalashnikova, A. M.; Rusakov, V. A.; Kaul, A. R.; Bayer, M.; Pisarev, R. V. *J. Appl. Phys.* **2012**, *111*, 056105.
(21) Akbashev, A. R.; Roddatis, V. V.; Vasiliev, A. L.; Lopatin, S.; Amelichev, V. A.; Kaul, A. R. *Sci. Rep.* **2012**, *2*, 672.
(22) Ahn, S.-J.; Lee, J.-H.; Jeong, Y. K.; Na, E.-H.; Koo, Y. M.; Jang, H. M. *Mater. Chem. Phys.* **2013**, *138*, 929.
(23) Masuno, A.; Sakai, S.; Arai, Y.; Tomioka, H.; Otsubo, F.; Inoue, H.; Moriyoshi, C.; Kuroiwa, Y.; Yu, J. *Ferroelectrics* **2009**, *378*, 169.
(24) Magome, E.; Moriyoshi, C.; Kuroiwa, Y.; Masuno, A.; Inoue, H. *Jpn. J. Appl. Phys.* **2011**, *49*, 09ME06.
(25) Zhou, J.-S.; Goodenough, J. B.; Gallardo-Amores, J. M.; Morán, E.; Alario-Franco, M. A.; Caudillo, R. *Phys. Rev. B* **2006**, *74*, 014422.
(26) Uusi-Esko, K.; Malm, J.; Imamura, N.; Yamauchi, H.; Karppinen, M. *Mater. Chem. Phys.* **2008**, *112*, 1029.
(27) Bréard, Y.; Fjellvåg, H.; Hauback, B. *Solid State Commun.* **2011**, *151*, 223.
(28) Nishibori, E.; Takata, M.; Kato, K.; Sakata, M.; Kubota, Y.; Oyagi, S. A.; Kuroiwa, Y.; Yamakata, M.; Ikeda, N. *Nucl. Instrum. Methods Phys. Res., Sect. A* **2001**, *467−468*, 1045.

(29) Tomuta, D. G.; Ramakrishnan, S.; Nieuwenhuys, G. J.; Mydosh, J. A. *J. Phys.: Condens. Matter* **2001**, *13*, 4543.
(30) Wu, C. T.; Lin, B. N.; Ku, H. C. *Chi. J. Phys.* **2003**, *41*, 652.
(31) Samal, S. L.; Green, W.; Lofland, S. E.; Ramanujachary, K. V.; Das, D.; Ganguli, A. K. *J. Solid State Chem.* **2008**, *181*, 61.